Electronic Supplementary Material (ESI) for Chemical Communications.
This journal is © The Royal Society of Chemistry 2023

Supporting Information

Cobalt Tris(4-Vinylphenyl)Corrole: Out of the Frying Pan into the Polymer

Nicolas Desbois,[a] W. Ryan Osterloh,[a] Dimitri Sabat,[a] Camille Monot,[a] Stéphane Brandès,[a] Michel Meyer,[a] Capucine Chaar,[b] Louise Hespel,[c] Laurent Lebrun,[c] Rachid Baati,[d] François Estour[b] and Claude P. Gros*[a]*

[a]*Université Bourgogne Franche-Comté, ICMUB (UMR CNRS 6302), Dijon, Cedex 21078, France. Email: claude.gros@u-bourgogne.fr*

[b]*Normandie Université, UNIROUEN, INSA Rouen, CNRS, COBRA (UMR 6014 & FR3038) 76000 Rouen, France. Email : francois.estour@univ-rouen.fr*

[c]*Normandie Univ., UNIROUEN, INSA ROUEN, CNRS, PBS, 76000 Rouen, France*

[d]*Université de Strasbourg, ICPEES, UMR CNRS 7515, 67087 Strasbourg, France*

Table of contents

1. Experimental

1.1. *Materials and instrumentation*

All the chemicals and solvents were purchased from commercial sources, unless otherwise stated, the reagents and solvents are directly used in the synthesis and testing procedures and required no further purification: pyrrole and magnesium sulfate ($MgSO_4$) were purchased from Sigma-Aldrich®. *p*-Chloranil and cobalt acetate tetrahydrate were purchased from Alfa Aesar®. Palladium(II) bis(triphenylphosphine) dichloride and 4-bromobenzaldehyde were purchased from Fluorochem. Potassium vinyltrifluoroborate was purchased from TCI, cesium carbonate from Fisher Scientific, and hydrazine from Acros®. Methanol (MeOH), ethanol (EtOH), dichloromethane (CH_2Cl_2), chloroform ($CHCl_3$), and tetrahydrofuran (THF) were purchased from Carlo ERBA®. Hydrochloric acid (HCl) (36%) was purchased from VWR chemicals®. Stabilizer-free THF was obtain from the solvent purification system (PureSolv) of Innovative Technology while the CH_2Cl_2 used for both the UV-visible and electrochemical titration was obtained from the same solvent system. Tetrabutylammonium perchlorate (TBAP, for electrochemical analysis, ≥99.0%) was purchased from Sigma-Aldrich® and used as received (**caution:** perchlorate salts are potentially explosive and should be handled with care). Column chromatography purification was carried out on silica gel (Silica 60, 40–63 μm Aldrich®). Analytical thin-layer chromatography (TLC) was carried out using Merck silica gel 60 F-254 plates (precoated sheets, 0.2 mm thick, with fluorescence indicator F254). For the polymerization process, anhydrous chloroform ($CHCl_3$), divinylbenzene (DVB) and azobisisobutyronitrile (AIBN) were purchased from Sigma-Aldrich®.

All spectrometers and diffractometers were available at the "Pôle de Chimie Moléculaire", the technological platform for chemical analysis and molecular synthesis (http://www.wpcm.fr) which relies on the Institute of the Molecular Chemistry of University of Burgundy and Welience™, a Burgundy University private subsidiary. ^1H spectra were acquired on a Bruker Avance III Nanobay 500 MHz spectrometer. Chemical shifts (δ) of proton were expressed in ppm relative to tetramethylsilane, using the residual proton peak of $CDCl_3$ (δ_H = 7.26 ppm) and DMSO-d_6 (δ_H = 2.50 ppm). Mass determination was run on a BRUKER Ultraflex II spectrometer in the MALDI/TOF reflectron mode using dithranol as matrix. High-resolution mass spectra (HRMS) were recorded on a LTQ Orbitrap XL (Thermo) instrument in the ESI mode.

All electrochemical measurements were carried out in CH_2Cl_2 solutions containing 0.1 M TBAP under an argon atmosphere by using an Autolab PGSTAT 302 N potentiostat,

connected to an interfaced computer that employed the Electrochemistry Nova software. The three-electrode system used for cyclic voltammetric measurements consisted of a glassy carbon working electrode, a platinum counter/auxiliary electrode, and a KCl-saturated calomel reference electrode (SCE) separated from the bulk of the solution by a fritted bridge of low porosity. Electrochemical titrations were performed in a similar fashion as the UV-vis titrations where a 10 μL microsyringe was used to deliver aliquots of titrant to the cell followed by purging the solution before recording the voltammogram.

1.2. *Spectrophotometric titrations*

UV-vis spectra in the 300-800 nm range were collected with a Cary 50 (Varian) spectrophotometer, using at 1.0 nm data interval and a 0.15 s integration time. A 1 cm Suprasil® cell (Hellma) filled with 3 mL of a 10^{-5} M corrole solution in CH_2Cl_2 was used to obtain the spectra. 5 μL aliquots of a stock ImA titrant solution (c = 0.718 and 1.06 mM in CH_2Cl_2 for experiment 1 and 2, respectively) were delivered to the corrole solution with a 10 μL microsyringe (Hamilton).

Data sets for two independent titrations were analyzed independently by a multiwavelength refinement with the Hypspec 2014 program,[1] which works by solving the mass-balance equations for the metal and ligand. The weighting scheme of $\omega_i = 1$ was used to process the data and the goodness-of-fit was assessed by the overall standard deviation of the residues (σ), a visual inspection of the residuals, and the physical meaning of the calculated electronic absorption spectra. Results for the two independent titrations are listed below. K_1 and K_2 stand for the successive apparent binding constants, respectively, while $\beta_1 = K_1$ and $\beta_2 = K_1K_2$ are the global equilibrium constants refined by the Hypspec 2014 program.

$$\mathbf{2Co} + \mathbf{ImA} \leftrightarrows \mathbf{2Co(ImA)} \qquad \beta_1 = [\mathbf{2Co(ImA)}]/[\mathbf{2Co}][\mathbf{ImA}]$$

$$\mathbf{2Co} + 2\,\mathbf{ImA} \leftrightarrows \mathbf{2Co(ImA)_2} \qquad \beta_2 = [\mathbf{2Co(ImA)_2}]/[\mathbf{2Co}][\mathbf{ImA}]^2$$

Experiment n°	log K_1	log β_2	log K_2	σ
1	7.97(3)	13.11(3)	5.14(2)	0.00408
2	8.17(4)	13.21(4)	5.04(5)	0.00196
Mean value	8.1(1)	13.16(9)	5.1(1)	

The calculated spectra for each of the three absorbing species in the 300–800 nm range shown in Fig. S1a match well those assigned for the titration (particularly the visible band at *ca.* 620 nm for **2Co(ImA)$_2$** consistent with six-coordinate corroles[2]). Moreover, the computed distribution diagram for these species obtained via the Hyss program[3] is depicted in Fig. S1b and shows that < 80% of **2Co(ImA)$_2$** is generated in the presence of 6.0 equiv of **ImA**, consistent with the electrochemical titration data shown in Fig. 2.

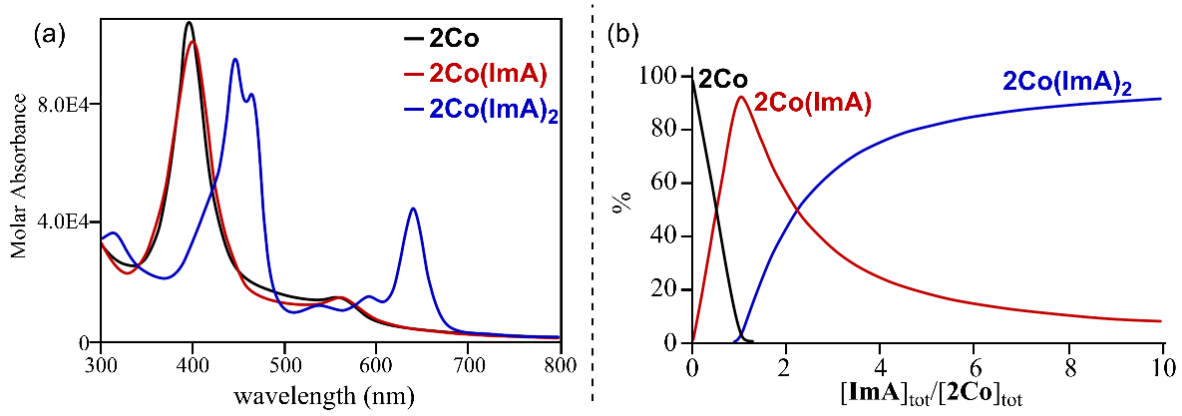

Fig. S1. (a) Calculated electronic spectra for **2Co** (black line), **2Co(ImA)** (red line) and **2Co(ImA)$_2$** (blue line). Solvent: CH_2Cl_2. (b) Computed species distribution curves for $[\mathbf{2Co}]_{Tot} = 1.05 \times 10^{-5}$ M, solvent: CH_2Cl_2.

1.3. *Electrochemical titrations*

Two independent electrochemical titrations were performed and afforded identical results as those shown in Fig. 1 and the assigned oxidation of **2Co(ImA)$_2$** at $E_{1/2}$ = 0.05 V was confirmed by the lack of observed current when applying a more negative potential (E_{app} = –0.2 V) than the half wave potential. It is also worth noting that the voltammograms recorded in the presence of 1.0 equiv. of **ImA** were obtained at lower temperature (0 °C) by dipping the cell into an ice water bath. This prevents complications stemming from a ligand exchange and finite electrical potential dependent equilibria. In short, the affinity of singly oxidized **2Co(ImA)** towards **ImA** is so large that [**2Co(ImA)**]$^+$ is able to purloin a second **ImA** ligand from a neighboring adduct, resulting in a mixture of [**2Co(L)$_2$**]$^+$ and [**2Co(ImA)$_2$**]$^+$ (ion-pair formation with L = ClO_4^- in CH_2Cl_2 is likely) leading to a messy current-voltage curve; whereas, measurements at low temp. curtail the rate of ligand exchange affording a reversible oxidation of **2Co(ImA)**.

a)

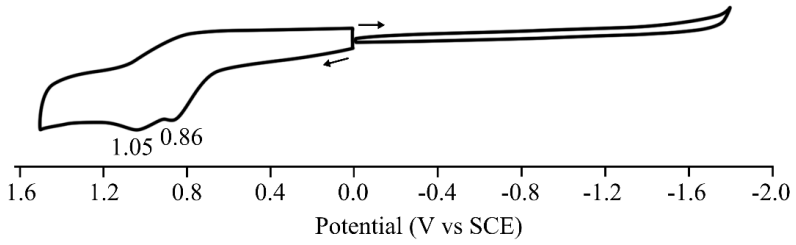

b)

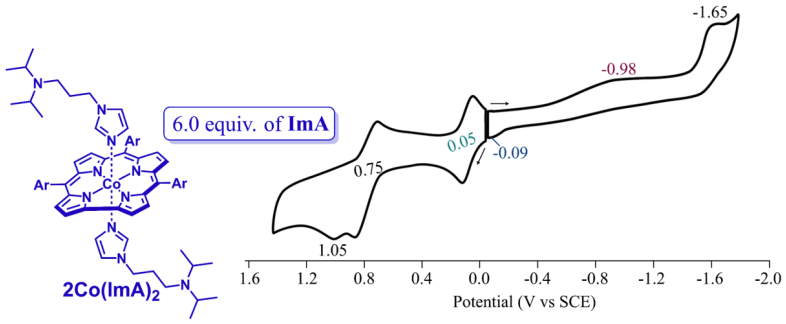

Fig. S2. a) Cyclic voltammograms of **ImA** (10^{-3} M) in CH_2Cl_2/0.1 M TBAP. Scan rate = 0.1 V/s. b) Cyclic voltammograms of **2Co(DMSO)** in CH_2Cl_2/0.1 M TBAP containing 6.0 equiv. of **ImA**.

Reductive scans of **2Co(ImA)$_2$** show a more complicated electron-transfer reaction. As seen in Fig. S2b), the initial negative potential sweep in the presence of 6.0 mol equiv. of **ImA** shows a first irreversible one-electron reduction at E_{pc} = –0.98 V *vs* SCE and is coupled to an anodic peak on the return potential sweep at E_{pa} = –0.09 V vs SCE. This latter value is identical to that observed for the same process prior to or after the addition of 1.0 equiv. **ImA** to solution, consistent with reoxidation of [**2Co**]$^-$ in each case. Overall, the electroreductive behavior for the first reduction is consistent with an electrochemical-chemical (EC) 'box-mechanism' where the E_{pc} and E_{pa} values are separated on the basis a kinetically controlled step associated with the electron transfer, similar to that described for six-coordinate bis-Py and mono-CN cobalt corroles.

2. Corrole Synthesis and Characterization

5,10,15-Tris(4-bromophenyl)corrole **1H$_3$**.[4] To a solution of 4-bromobenzaldehyde (3.00 g, 16.21 mmol) in MeOH (650mL) and water (650 mL) was added pyrrole (2.0 equiv., 2.25 mL, 32.42 mmol) and hydrochloric acid 36% (13.43 mL). The solution was stirred at r.t for 3 h in the dark. The product was extracted with $CHCl_3$ twice and the organic phase was washed with water twice. The organic phase was partially evaporated and *p*-chloranil (4.00 g, 16.21 mmol) was added to the solution. The mixture was refluxed for 1 h and evaporated. Hot EtOH was added and the precipitate product was filtered. The obtained powder was washed with cold CH_2Cl_2 then purified by a gel silica plug using a neat CH_2Cl_2 eluent. The product was finally obtained as a dark green solid. Yield: 7.3%, 302.6 mg. UV-Vis (CH_2Cl_2) λ_{max} (nm) ($\varepsilon \times 10^{-3}$ L mol^{-1} cm^{-1}): 416.0 (129), 576.0 (3.7), 620.0 (3.2), 648.0 (2.8). ^{1}H NMR (500 MHz, DMSO-d_6 + 10 µL hydrazine) δ (ppm): 8.95 (d, J = 4.0 Hz, 2H$_ß$), 8.63 (d, J = 4.5 Hz, 2H$_ß$), 8.51 (d, J = 4.0 Hz, 2H$_ß$), 8.31 (d, J = 4.5 Hz, 2H$_ß$ H), 8.19 (d, J = 8.0 Hz, 4H$_{Ph}$), 8.02 (d, J = 8.0 Hz, 2H$_{Ph}$), 7.97 (d, J = 8.0 Hz, 4H$_{Ph}$), 7.89 (d, J = 7.9 Hz, 2H$_{Ph}$). LRMS (MALDI/TOF) m/z calcd for $C_{37}H_{23}N_4Br_3$: 761.94 $[M]^{+\bullet}$; found: 761.55.

5,10,15-Tris(4-vinylphenyl)corrole **2H$_3$**. To a solution of corrole **1H$_3$** (50.0 mg, 0.066 mmol) in toluene (20 mL) were added potassium vinyltrifluoroborate (70.0 mg, 0.53 mmol, 8 equiv.), cesium carbonate (173 mg, 0.53 mmol, 8 equiv.) and palladium(II) bis(triphenylphosphine)dichloride (4.0 mg, 0.006 mmol, 0.1 equiv.), followed by water (10 mL). The reaction was stirred under reflux and under argon during 36 h. At room temperature, toluene was evaporated and water (20 mL) was added and the product was extracted with CH_2Cl_2 twice. The organic phase was washed with water and brine twice, dried over $MgSO_4$ and evaporated. The crude product was purified twice on a silica plug with CH_2Cl_2/Heptane (7/3) and recrystallized with EtOH. **2H$_3$** was isolated after solvent evaporation as a green powder. Yield: 41%, 16.3 mg. UV-Vis (CH_2Cl_2) λ_{max} (nm) ($\varepsilon \times 10^{-3}$ L mol^{-1} cm^{-1}): 426 (102.1), 583 (17.0), 623 (15.2), 666 (15.2). ^{1}H NMR (500 MHz, DMSO-d_6 + 10 µL hydrazine) δ (ppm): 8.98 (d, J = 4.0 Hz, 2H$_ß$), 8.70 (d, J = 4.5 Hz, 2H$_ß$), 8.56 (d, J = 4.0 Hz, 2H$_ß$), 8.37 (d, J = 4.5 Hz, 2H$_ß$), 8.28 (d, J = 7.8 Hz, 4H$_{Ph}$), 8.11 (d, J = 7.8 Hz, 2H$_{Ph}$), 7.94 (d, J = 7.8 Hz, 4H$_{Ph}$), 7.86 (d, J = 7.8 Hz, 2H$_{Ph}$), 7.09 (m, 3H$_{vinyl}$), 6.13 (d, J_{trans} = 17.5 Hz, 3H$_{vinyl}$), 5.50 (d, J_{cis} = 11.0 Hz, 3H$_{vinyl}$). LRMS (MALDI/TOF) m/z calcd for $C_{43}H_{33}N_4$: 605.27 $[M+H]^+$; found: 605.25. HRMS (ESI) m/z calcd for $C_{43}H_{33}N_4$: 605.2700 $[M+H]^+$; found: 605.2697.

Cobalt 5,10,15-Tris(4-vinylphenyl)corrole **2Co(DMSO).** To a solution of corrole **2H**$_3$ (40.4 mg, 0.058 mmol) in DMSO (8.6 mL) was added $Co(OAc)_2.4H_2O$ (20.2 mg, 0.081 mmol, 1.4 equiv.). The solution was stirred and heated at 80 °C for 40 min. After the completion of the reaction, the solution was cooled at r.t and cold brine (30 mL) was added to precipitate the corrole. The precipitate was collected by centrifugation and washed with water. This procedure was repeated 5 times and the product was dried under vacuum overnight. Yield 98%, 45.3 mg. UV-Vis (CH_2Cl_2) λ_{max} (nm) ($\varepsilon \times 10^{-4}$ L mol^{-1} cm^{-1}): 395 (10.1), 554 (1.5). ^{1}H NMR (500 MHz, $CDCl_3$ + $NH_{3(g)}$) δ (ppm): 9.21 (d, J = 4.0 Hz, 2H$_ß$), 9.06 (d, J = 5.0 Hz, 2H$_ß$), 8.86 (m, 4H$_ß$), 8.30 (d, J = 7.5 Hz, 4H$_{Ph}$), 8.21 (d, J = 7.5 Hz, 2H$_{Ph}$), 7.84 (d, J = 7.5 Hz, 4H$_{Ph}$), 7.80 (d, J = 7.5 Hz, 2H$_{Ph}$), 7.06 (dd, J_{cis} = 11.0 Hz, J_{trans}= 18 Hz, 3H$_{vinyl}$), 6.5 (d, J_{trans}= 18.0 Hz, 3H$_{vinyl}$), 5.45 (d, J_{cis}=11.0 Hz, 3H$_{vinyl}$), 2.62 (s, 6H$_{DMSO}$), –6.75 (s, 6H$_{NH_3}$). LRMS (MALDI/TOF) m/z calcd for $C_{43}H_{29}N_4Co$: 660.17 $[M–DMSO]^{+\bullet}$; found: 660.18. HRMS (ESI) m/z calcd for $C_{43}H_{29}N_4Co$: 660.1719 $[M–DMSO]^{+\bullet}$; found: 660.1718.

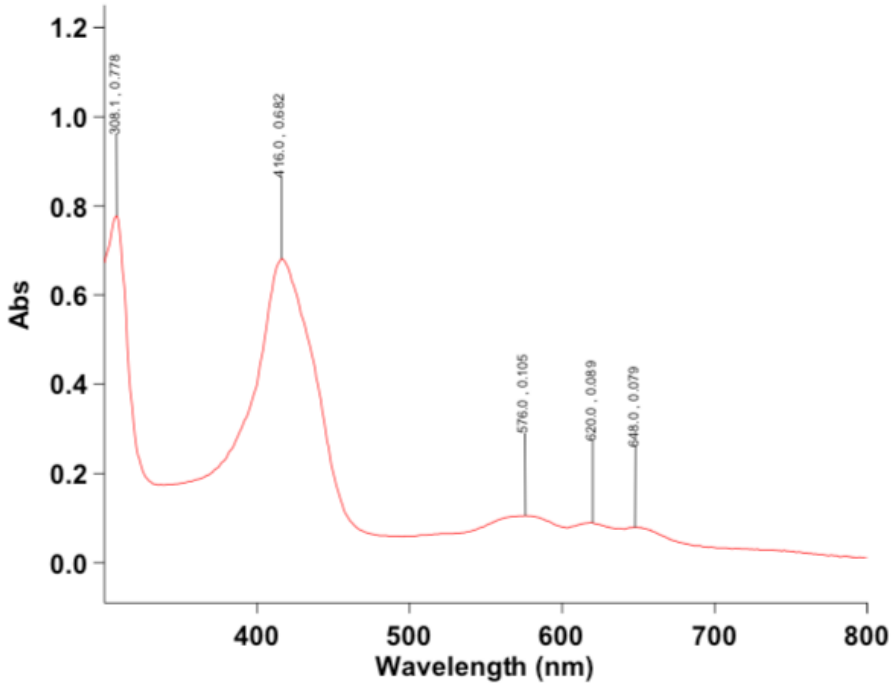

Figure S3. UV-visible spectrum of **1H₃** in CH_2Cl_2.

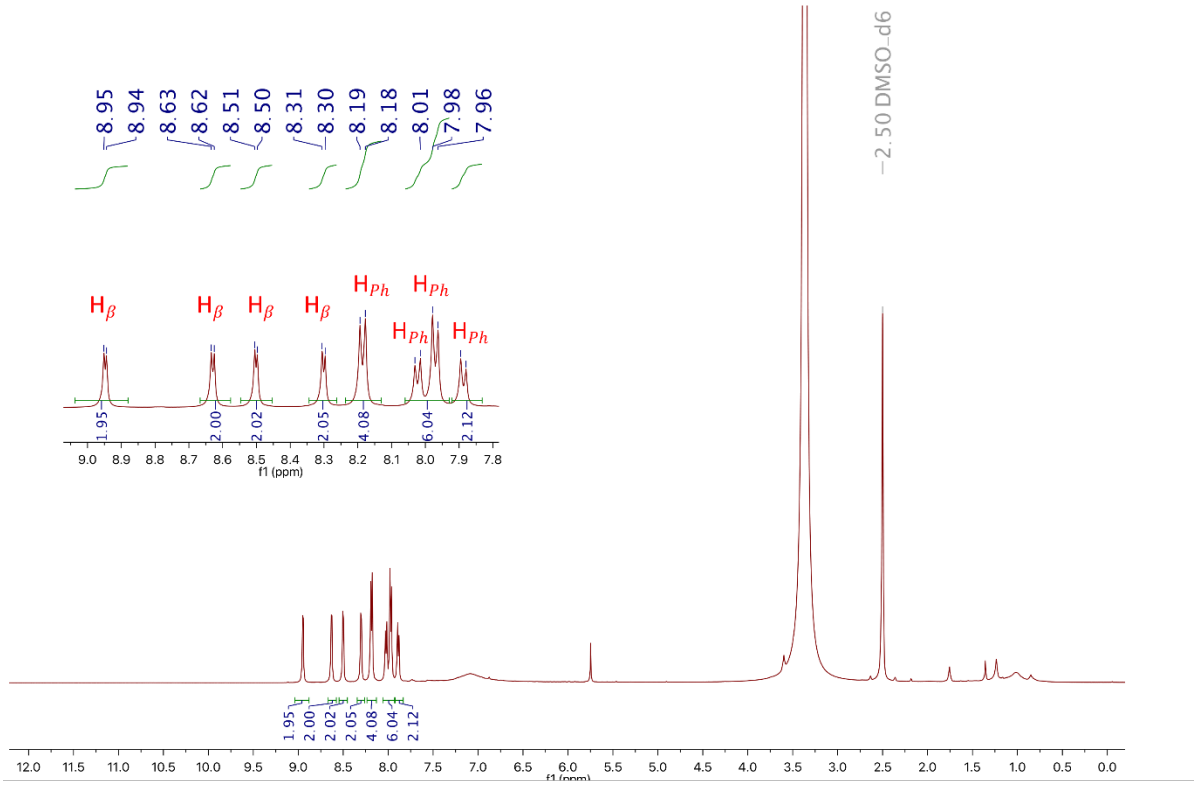

Figure S4. ^{1}H NMR spectrum (500 MHz) of **1H₃** in $CDCl_3$ (+ hydrazine).

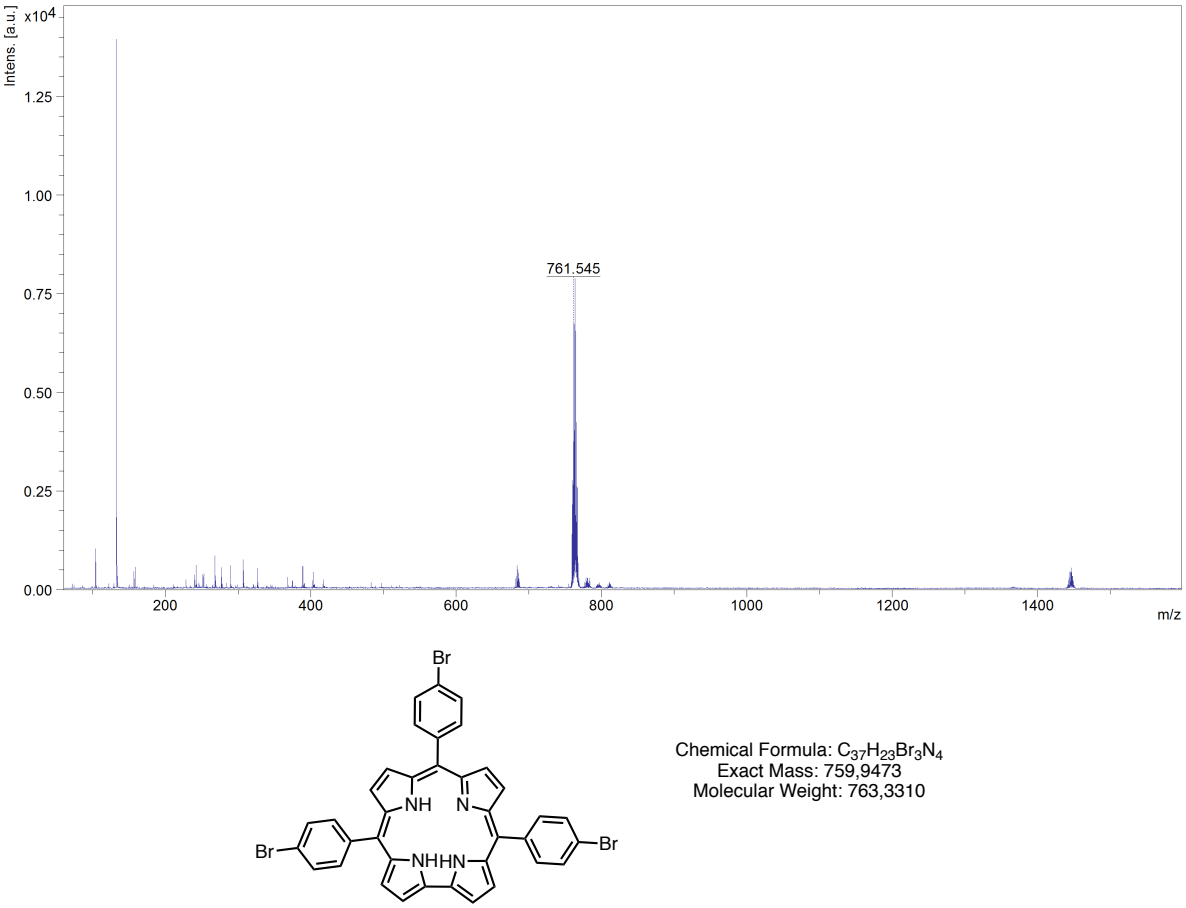

Figure S5. MALDI-TOF LRMS mass spectrum of **1H$_3$**.

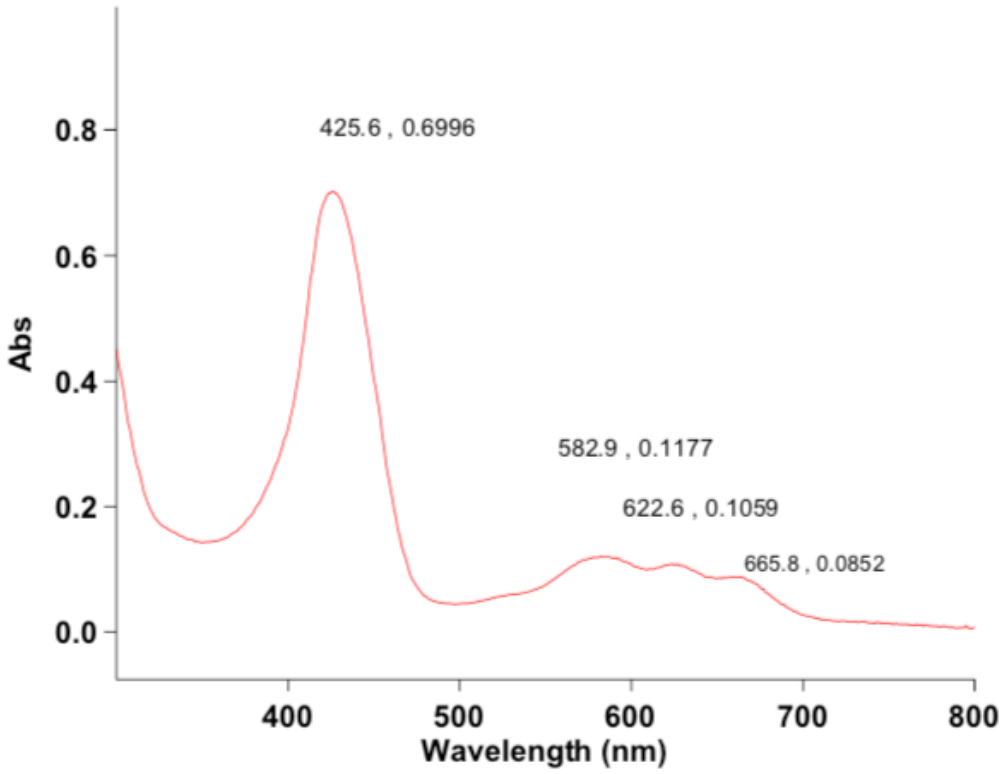

Figure S6. UV-visible spectrum of **2H₃** in CH_2Cl_2.

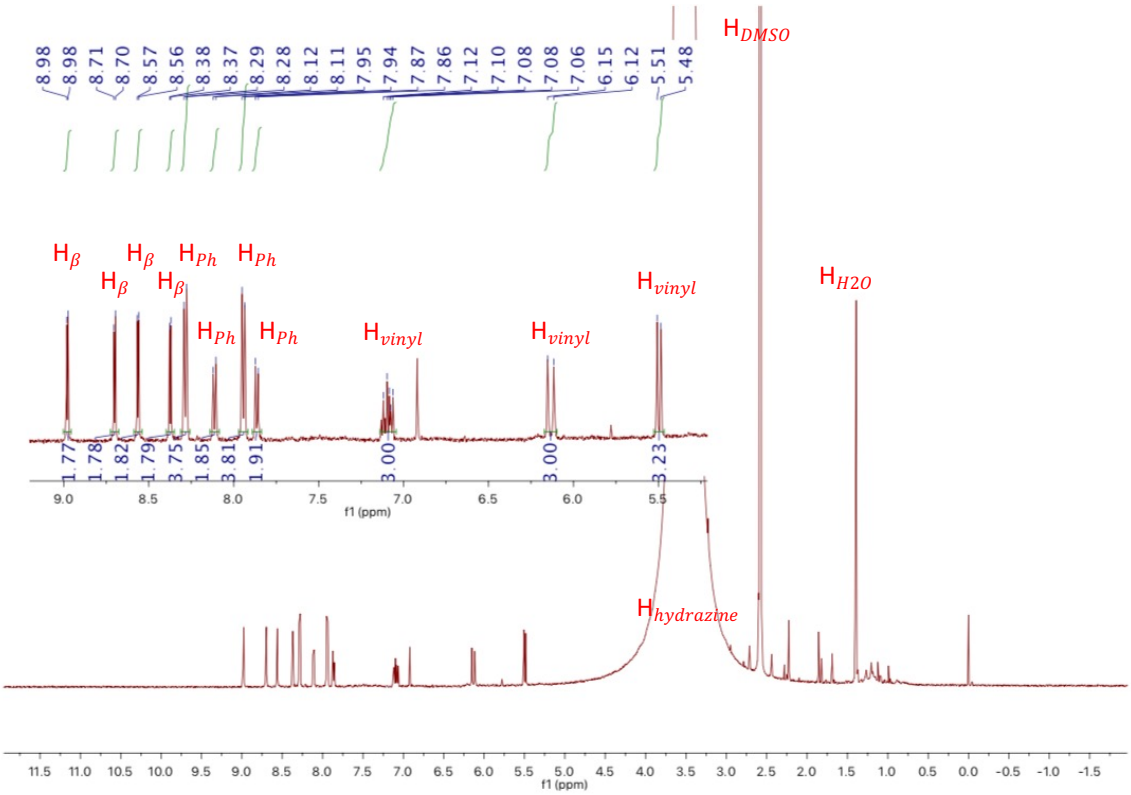

Figure S7. ^{1}H NMR spectrum (500 MHz) of **2H₃** in $CDCl_3$ (+ hydrazine).

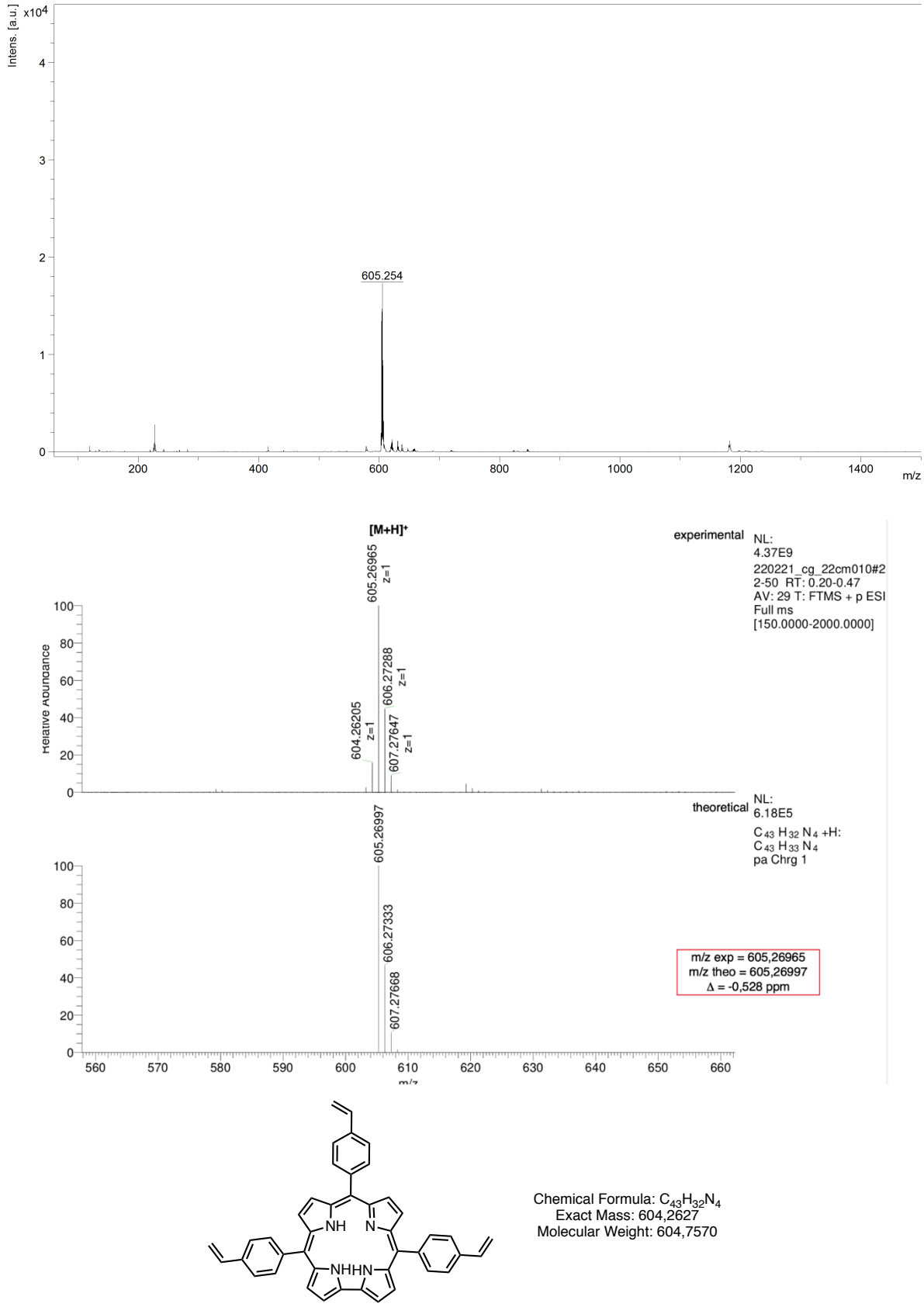

Figure S8. MALDI-TOF LRMS and ESI HRMS mass spectra of **2H$_3$**.

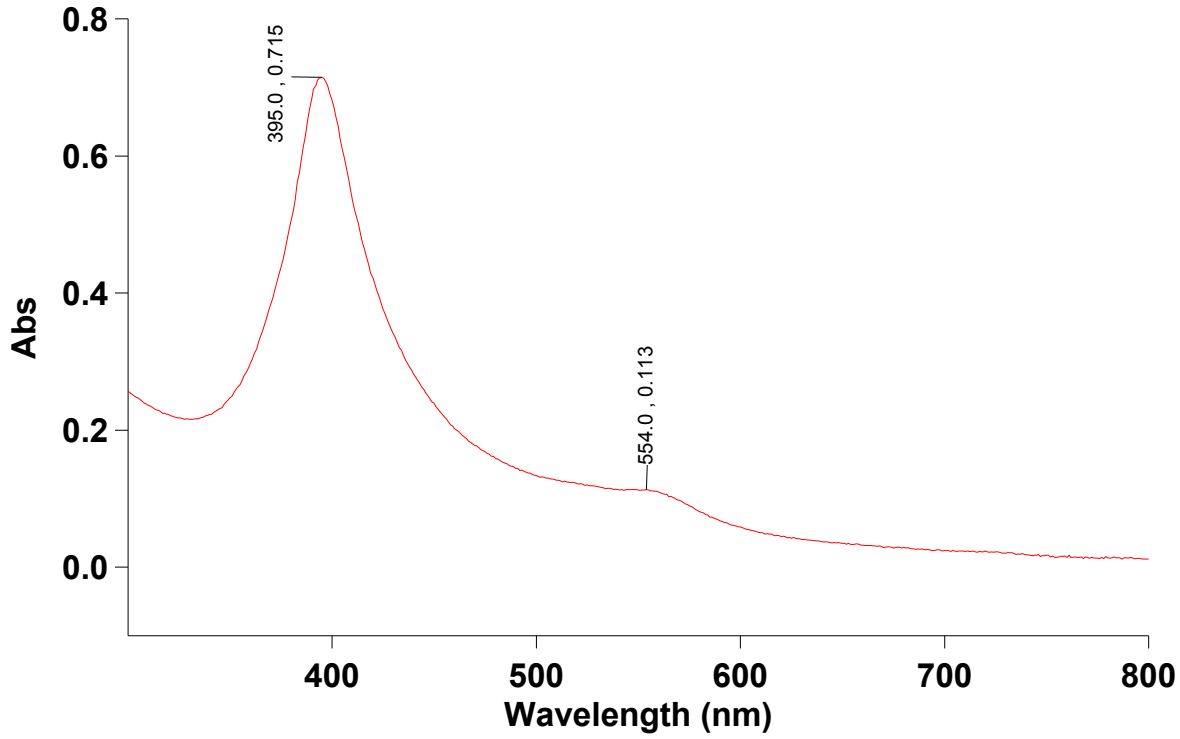

Figure S9. UV-visible spectrum of **2Co(DMSO)** in CH_2Cl_2.

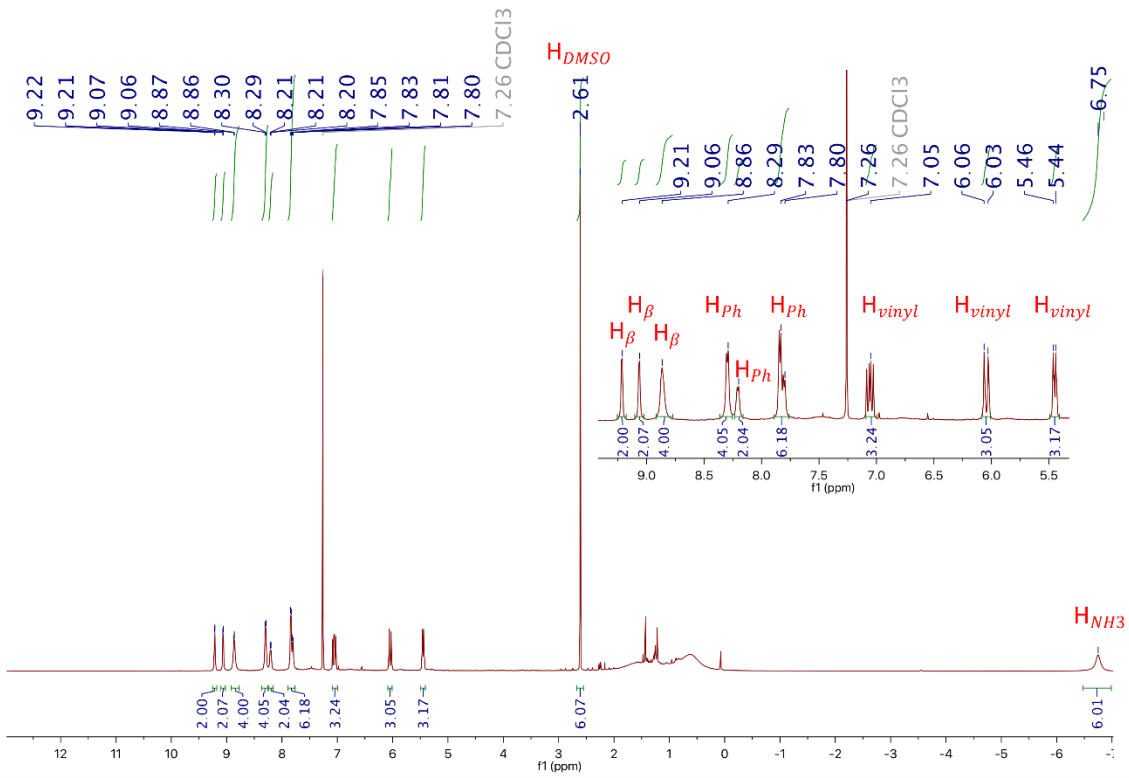

Figure S10. ^{1}H NMR spectrum (500 MHz) of **2Co(DMSO)** in $CDCl_3$ (+ $NH_{3(g)}$)

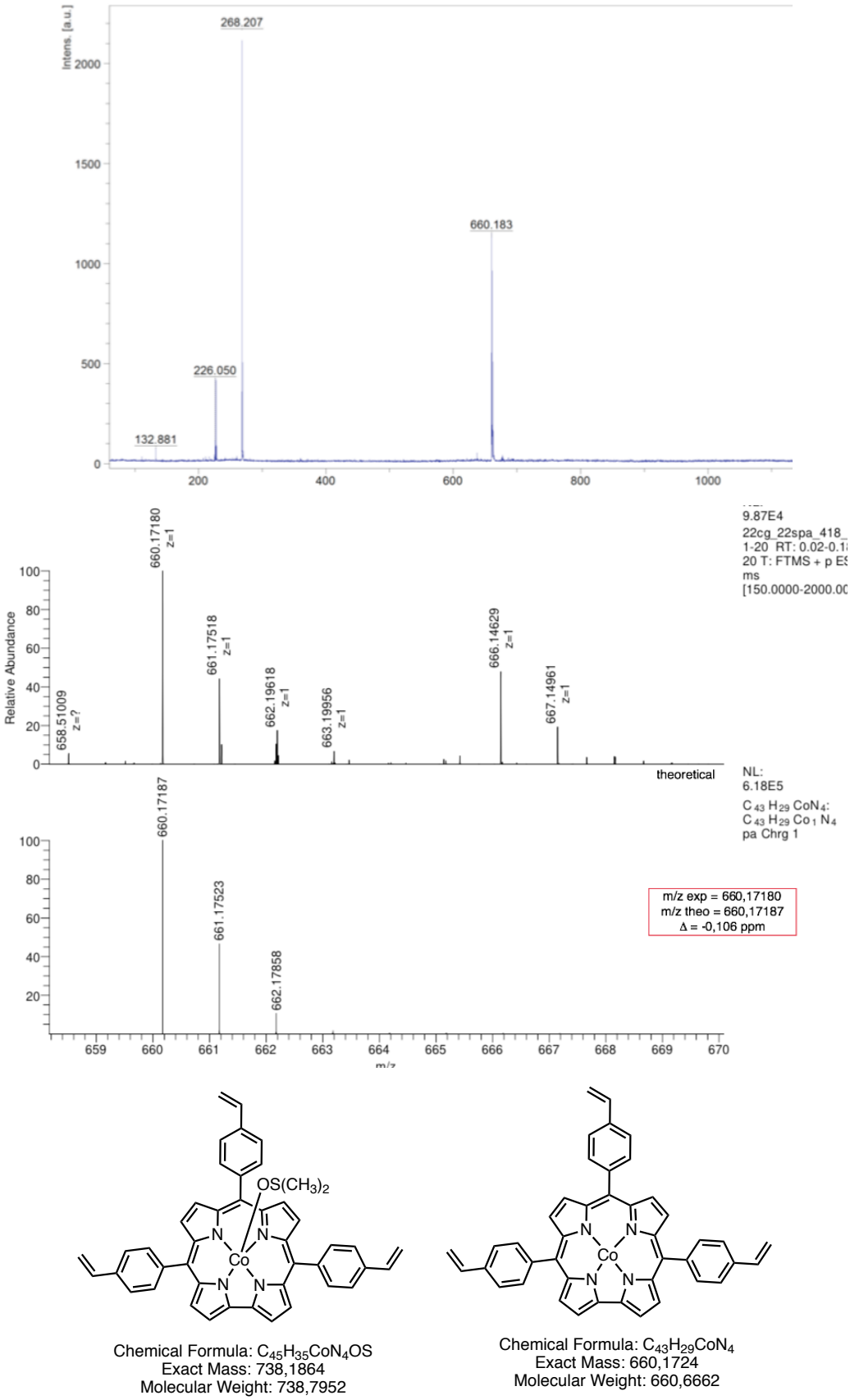

Figure S11. MALDI-TOF LRMS and ESI HRMS mass spectra of **2Co(DMSO)**.

3. Polymer synthesis and characterization

3.1. *Synthesis of the polymer incorporating the **2Co(DMSO)** corrole*

2Co(DMSO) (2.4 µmol, 1.8 mg, 1 equiv.), DVB (1.03 µmol, 150 µL, 432 equiv.) and AIBN (13 µmol, 2.2 mg, 5.5 equiv.) were dissolved in 1 mL of dried chloroform at room temperature under argon atmosphere. Then the vial was sealed and the reaction mixture was stirred for 18 h at 65 °C. Finally, the resulting polymer was thoroughly washed four times with 15 mL of chloroform before being crushed. The polymerization reaction afforded a black powder with a yield of 59%.

3.2. *Synthesis of the reference polymer*

DVB (1.03 µmol, 150 µL, 67 equiv.) and AIBN as radical (15 µmol, 2.5 mg, 1 equiv.) were dissolved in 1 mL of dried chloroform at room temperature under argon atmosphere. Then the vial was sealed and the reaction mixture was stirred for 18 h at 65 °C. Finally, the resulting polymer was thoroughly washed four times with 15 mL of chloroform before being crushed. The polymerization reaction lead to a white powder with a yield of 93%.

a) b)

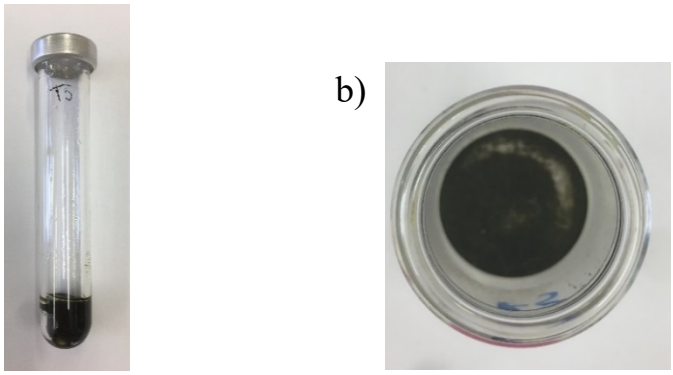

Figure S12. Pictures showing the polymer obtained with **2Co(DMSO)** a) before crushing in the sealed reaction tube and b) after grinding and sieving the crude polymer.

a) b)

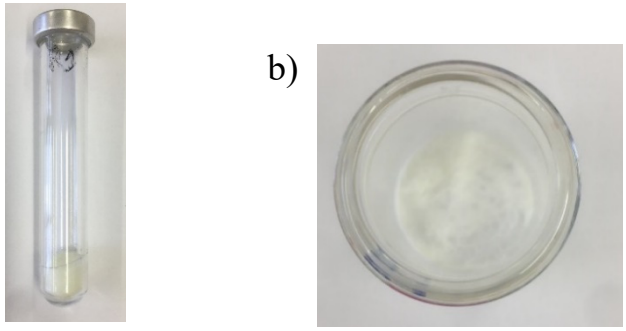

Figure S13. Pictures showing the reference polymer obtained in the absence of corrole a) before crushing in the sealed reaction tube and b) after grinding and sieving the crude polymer.

3.3. *Microscopy observations*

Surface morphologies of the polymer particles were observed by scanning electron microscopy (SEM) coupled with an EDX analyzer using the SEM EVO40EP from Zeiss. The samples were first covered with a thin layer of carbon before study.

Particles were also observed by Transmission Electron Microscopy (TEM) using a double corrected analytical TEM Jeol ARM 200 employed in STEM-HAADF mode for imaging and EDS elemental mapping (Centurio 100 mm^2 EDS detector). Images were acquired on more than 20 areas and EDS chemical analysis was carried out for three separate representative areas within the sample. For each region, the EDS maps were acquired for at least 60 min. Before examination, the samples were mechanically pulverised, and the size of the particles was reduced and dispersed under ultrasound for 5 min in pure ethanol. Three drops of solution were deposited on a holey carbon membrane deposited on a 300 mesh Au grid for observation.

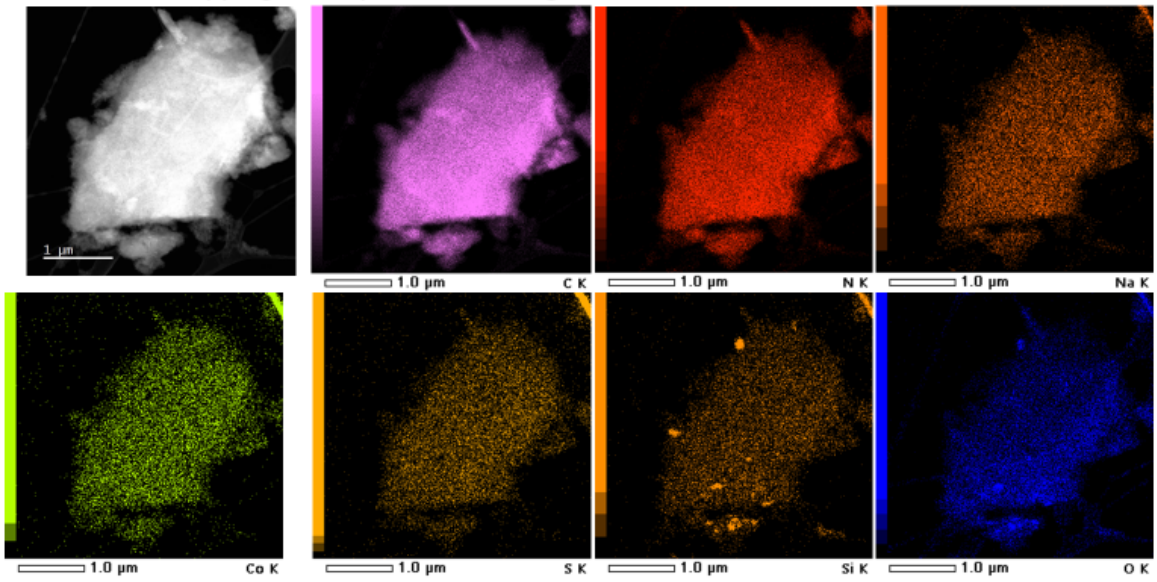

Figure S14: Elemental mapping of a particle representative region.

3.4. *Inductively Coupled Plasma Mass Spectrometry (ICP-MS)*

The sample was mixed with 5 mL of 68% nitric acid in a Teflon reactor. The mixture was brought to 180 °C for 30 min in a Milestone ETHOS 1 microwave oven. After cooling, the extract was added to a 50 mL flask adjusted with ultrapure water. The obtained solution was then centrifuged for 2 min at 4000 rpm then diluted to 1:100 using ultrapure water before the ICP-MS analysis (ICP-MS "ICAP RQ" THERMO controlled by the Qtegra software) in STD mode.

4. References

1. P. Gans, A. Sabatini and A. Vacca, *Talanta*, 1996, **43**, 1739-1753.

2. (a) W. Sinha, A. Mizrahi, A. Mahammed, B. Tumanskii and Z. Gross, *Inorg. Chem.*, 2018, **57**, 478-485; (b) L. Lvova, G. Pomarico, F. Mandoj, F. Caroleo, C. Di Natale, K. M. Kadish and S. Nardis, *J. Porphyrins Phthalocyanines*, 2020, **24**, 964-972; (c) S. Ooi, B. Adinarayana, D. Shimizu, T. Tanaka and A. Osuka, *Angew. Chem. Int. Ed.*, 2020, **59**, 9423-9427; (d) H. M. Rhoda, L. A. Crandall, G. R. Geier, C. J. Ziegler and V. N. Nemykin, *Inorg. Chem.*, 2015, **54**, 4652-4662; (e) Jyoti, N. Fridman, A. Kumar and S. G. Warkar, *Inorg. Chim. Acta*, 2021, **527**, 120580; (f) S. Ooi, T. Tanaka and A. Osuka, *J. Porphyrins Phthalocyanines*, 2016, **20**, 274-281; (g) K. M. Kadish, J. Shen, L. Frémond, P. Chen, M. El Ojaimi, M. Chkounda, C. P. Gros, J.-M. Barbe, K. Ohkubo, S. Fukuzumi and R. Guilard, *Inorg. Chem.*, 2008, **47**, 6726-6737; (h) K. M. Kadish, J. Shao, Z. Ou, C. P. Gros, F. Bolze, J.-M. Barbe and R. Guilard, *Inorg. Chem.*, 2003, **42**, 4062-4070; (i) S. Ganguly, J. Conradie, J. Bendix, K. J. Gagnon, L. J. McCormick and A. Ghosh, *J. Phys. Chem. A*, 2017, **121**, 9589-9598; (j) V. Quesneau, W. Shan, N. Desbois, S. Brandès, Y. Rousselin, M. Vanotti, V. Blondeau-Patissier, M. Naitana, P. Fleurat-Lessard, E. Van Caemelbecke, K. M. Kadish and C. P. Gros, *Eur. J. Inorg. Chem.*, 2018, **2018**, 4265-4277; (k) X. Jiang, M. L. Naitana, N. Desbois, V. Quesneau, S. Brandès, Y. Rousselin, W. Shan, W. R. Osterloh, V. Blondeau-Patissier, C. P. Gros and K. M. Kadish, *Inorg. Chem.*, 2018, **57**, 1226-1241; (l) K. Sudhakar, A. Mahammed, N. Fridman and Z. Gross, *Dalton Trans.*, 2019, **48**, 4798-4810; (m) W. R. Osterloh, N. Desbois, V. Quesneau, S. Brandès, P. Fleurat-Lessard, Y. Fang, V. Blondeau-Patissier, R. Paolesse, C. P. Gros and K. M. Kadish, *Inorg. Chem.*, 2020, **59**, 8562-8579; (n) N. I. Neuman, U. Albold, E. Ferretti, S. Chandra, S. Steinhauer, P. Rößner, F. Meyer, F. Doctorovich, S. E. Vaillard and B. Sarkar, *Inorg. Chem.*, 2020, **59**, 16622-16634; (o) W. R. Osterloh, V. Quesneau, N. Desbois, S. Brandès, W. Shan, V. Blondeau-Patissier, R. Paolesse, C. P. Gros and K. M. Kadish, *Inorg. Chem.*, 2020, **59**, 595-611.

3. L. Alderighi, P. Gans, A. Ienco, D. Peters, A. Sabatini and A. Vacca, *Coord. Chem. Rev.*, 1999, **184**, 311-318.

4. B. Koszarna and D. T. Gryko, *J. Org. Chem.*, 2006, **71**, 3707-3717.